

Dynamic Evolution of Droplet/Particle Size Distribution in Suspension Polymerization of Styrene

*H. Farahzadi, M. Shahrokhi**

Department of Chemical and Petroleum Engineering, Sharif University of Technology, Tehran, Iran

Abstract

In the present work, a population balance model is used to predict dynamic evolution of droplet/particle size distribution in non-reactive liquid-liquid dispersions and reactive liquid (solid)-liquid suspension polymerization systems. The effect of dispersed phase hold-up and agitation rate on droplet/particle size and droplet/particle size distribution are investigated. The cell average technique is applied for solving the population balance equation. Predictive capability of the presented model is demonstrated by comparison of model predictions with experimental data regarding the average mean diameter for non-reactive liquid-liquid dispersions and the free-radical suspension polymerization of styrene.

Keywords: *Population Balance model, Suspension Polymerization, Cell average Technique, Polystyrene*

1- Introduction

Suspension polymerization is commonly used for producing wide varieties of commercially important polymers such as polystyrene and its copolymers, poly methyl methacrylate, poly vinyl chloride and etc. In suspension polymerization, the monomer is initially dispersed in the continuous aqueous phase by a combined action of surface-active agents (i.e., inorganic or/and water soluble polymers) and agitation. Polymerization occurs in the monomer droplets that are progressively transformed into sticky, viscous monomer-polymer particles and finally into rigid, spherical polymer particles

of size 50-500 μm [1]. An important property of suspension polymerization processes is the particle size distribution (PSD), which controls key aspects of the process and affects the end-use properties of the product.

Suspension polymerization processes are generally characterized by PSD that can vary with time with respect to the mean particle size as well as to the PSD form. The quantitative calculation of the evolution of PSD provides a good knowledge of the droplet/particle breakage and coalescence mechanisms. These mechanisms coupled with the reaction kinetics, thermodynamics

* Corresponding author: shahrokhi@sharif.ir

and other microscale phenomena, including mass and heat transfer between different phases, describe the system behaviour. The time evolution of PSD is commonly obtained from the solution of a population balance equation (PBE), governing the dynamic behaviour of the dispersed liquid monomer droplets that are being polymerized to solid polymer particles [2]. In comparison with the number of studies appearing in the literature on kinetics of polymerization and/or properties of final polymer particles, less attention has been paid to the study of evolution of particle size and PSD. The main reason is perhaps the complexity of phenomena that determines the particle size.

In principle, a balance between the rate of drop breakage and coalescence determines the size of the drops in suspension polymerization. Therefore, the drop size is a strong function of several parameters such as the densities and viscosities of continuous and dispersed phases, interfacial tension, the type and concentration of the suspending agent, dispersed phase hold up, type of impeller and stirring speed, as well as the kinetics of polymerization [3].

In this work, based on the population balance model, the dynamic evolution of droplet/particle size distribution in non-reactive and reactive liquid-liquid dispersion systems is predicted. Effects of dispersed phase hold-up and agitation rate on droplet/particle size and droplet/particle size distribution are investigated. The cell average technique is applied for solving the population balance equation. Simulation results are evaluated by comparing them with the experimental data.

2- Process model

A number of mathematical models have been reported for suspension polymerization systems. These models consider the effects of viscoelastic properties of polymerizing drops on the rates of drop breakage and coalescence [1, 4, 5], as well as the nonhomogeneity of the turbulent flow [6].

A mathematical model, based on population balance equation (PBE), is used to describe the system dynamics. The tank Reynolds number for all conditions is above 10^4 , implying a fully developed turbulent flow in the system. A homogeneous turbulent flow during the suspension polymerization was assumed. In the applied model the evaluation of drop volume distribution has been carried out by the numerical solution of the PBE for the dispersed drops. The distribution of the droplets/particles is considered to be continuous in the volume domain and is usually described by a number density function, $n(V,t)$. Thus, $n(V,t)dV$ represents the number of particles per unit volume in the differential volume size range $(V, V+dV)$. For a dynamic particulate system undergoing simultaneous particle breakage and coalescence, the rate of change of number density function with respect to time and volume is given by the following non-linear integro-differential equation:

$$\begin{aligned} \frac{\partial [n(V,t)]}{\partial t} = & \int_V^{V_{\max}} \beta(U,V)u(U)g(U)n(U,t)dU \\ & + \int_{V_{\min}}^{V/2} k(V-U,U)n(V-U,t)n(U,t)dU \\ & - n(V,t)g(V) - n(V,t) \int_{V_{\min}}^{V_{\max}} k(V,U)n(U,t)dU \end{aligned} \quad (1)$$

$\beta(U, V)$ is a daughter drop breakage function, accounting for the probability that a drop of volume V is formed via the breakage of a drop of volume U . The function $u(U)$ denotes the number of droplets formed by the breakage of a drop of volume U . $g(U)$ is the breakage rate of the drops of volume U , and $k(V, U)$ is the coalescence rate between two drops of volume V and U .

2.1- Breakage and coalescence rates

In the open literature, several forms of $g(V)$ and $k(V, U)$ have been proposed to describe the drop breakage and coalescence rate functions in liquid-liquid dispersions. According to modifications proposed by Maggioris et al. [6], the breakage and coalescence rates can be expressed in terms of the breakage, ω_b , and collision, ω_c , frequencies and the respective Maxwellian efficiencies, λ_b and λ_c :

$$g(V) = \omega_b(V) e^{-\lambda_b(V)} \quad (2)$$

$$k(V, U) = \omega_c(V, U) e^{-\lambda_c(V, U)} \quad (3)$$

λ_b and λ_c denote the corresponding ratios of required energy to available energy for an event to occur. In the present study, the breakage of a drop exposed to a turbulent flow field was supposed to occur as result of the energy transfer from the eddy to a drop having a diameter equal to the eddy wave length, D_v . Eddy fluctuations with wave lengths smaller (larger) than the drop diameter D_v produce an oscillatory (rigid body) motion of the drop that does not lead to breakage [4]. The frequency term is given by:

$$\omega_b(V) = \bar{u}(D_v) / D_v \quad (4)$$

where $\bar{u}(D_v)^2$ is the mean square of the relative velocity between two points separated by a distance D_v , or the mean square fluctuation velocity of drops of diameter D_v . In the inertial subrange of turbulence and viscous dissipation range, $\bar{u}(D_v)^2$ is given by the following equations:

$$\bar{u}(D_v)^2 = k_b (\varepsilon_s D_v)^{2/3} \quad \text{if } \eta < D_v \ll L \quad (5)$$

$$\bar{u}(D_v)^2 = k_b D_v^2 (\varepsilon_s / \nu_c) \quad \text{if } D_v < \eta \quad (6)$$

where η is the microscale of turbulence and L is the macroscale of turbulence and can be approximated by the width of the fluid ejected by the agitator, i.e. the width of the impeller blade. Considering that the flow within a drop can be described as a one-dimensional simple-shear flow of a Maxwellian fluid, the following expression was derived for breakage efficiency [1]:

$$\lambda_b(V) = a_b \Omega(D_v) = a_b \left(\frac{2}{\text{Re}(D_v) [1 + \text{Re}(D_v) V_e(D_v)]} + \frac{Cd_s}{We(D_v)} \right) \quad (7)$$

Elasticity is accounted by the dimensionless quantity V_e which is a function of the Reynolds number and can be determined from the following equation:

$$V_e(D_v) = \Theta \exp \left[-\frac{1-\alpha}{2Y_0 \text{Re}(D_v)} \right] - \frac{1}{12} \quad (8)$$

where

$$\alpha = \sqrt{1 - 48Y_0} \quad (9)$$

$$Y_0 = \frac{\mu_d^2}{\rho_d E_d D_v^2} \quad (10)$$

and

$$\Theta = \frac{Y_0}{\alpha(1-\alpha)} \left[1 + \alpha - \frac{(1-\alpha)^2}{1+\alpha} \exp\left(-\frac{1-\alpha}{2Y_0 \text{Re}(D_v)}\right) \right] \quad (11)$$

The dispersed phase elasticity modulus, E_d , can be defined as a function of the polymer elasticity modulus E_p and conversion as the following expression:

$$E_d = \chi E_p \quad (12)$$

The scalar quantity Cd_s in equation (7) can be expressed in terms of numbers and volumes of daughter and satellite drops:

$$Cd_s = \frac{N_{da} r^{2/3} + N_{sa}}{(N_{da} r + N_{sa})^{2/3}} - 1, \quad r = \frac{V_{da}}{V_{sa}} \quad (13)$$

where N_{da} is the number of daughter drops of volume V_{da} and N_{sa} is the number of satellite drops of volume V_{sa} . In the present study, the number of daughter drops was set equal to 2, the volume ratio of daughter to satellite drops, r , was considered to be constant, while the number of satellite drops was calculated as a function of the parent drop size:

$$N_{sa} = \text{integer}(S_{nsa} D_u^{1/3}) \quad (14)$$

The breakage distribution function can be considered as a result of a large number of

independent random events and therefore, the drop size distribution can be assumed normally distributed. Thus, for a binary breakage the droplet rupture functions, i.e., the number of drops per breakage and the breakage distribution function, are [8]:

$$u(U) = 2 \quad (15)$$

$$\beta(U, V) = \frac{2.4}{V} \exp\left(-4.5 \frac{(2U - V)^2}{V^2}\right)$$

with a variance such that 99.6% of the daughter drop distribution lies on the $(0, V)$ intervals.

Assuming that the drop collision mechanism in a locally isotropic flow field is analogous to collisions between molecules as in the kinetic theory of gases. The collision frequency between two drops with volume V and U can be expressed as [6]:

$$\omega_c(V, U) = K_c (D_v^2 + D_u^2) \sqrt{\bar{u} (D_v)^2 + \bar{u} (D_u)^2} \quad (16)$$

For drops in the inertial subrange of turbulence, by using Eq. (5), the last expression can be written as:

$$\omega_c(V, U) = k_c \varepsilon_s^{1/3} (D_v^2 + D_u^2) \sqrt{D_v^{2/3} + D_u^{2/3}} \quad (17)$$

For droplets in the viscous dissipation range, substitution of Eq. (6) into Eq. (17) yields:

$$\omega_c(V, U) = k_c (\varepsilon_s / \nu_c)^{1/2} (D_v^2 + D_u^2)^{3/2} \quad (18)$$

According to reference [8], for deformable drops, which is generally the case for low interfacial tension dispersions or large-size

drops, the drop coalescence efficiency can be expressed as:

$$\lambda_c^{(\alpha)}(V, U) = \exp\left(-a_c \frac{\mu_c \rho_c \varepsilon_s}{\sigma^2} \left[\frac{D_v D_u}{D_v + D_u}\right]^4\right) \quad (19)$$

where a_c is a model parameter and μ_c , ρ_c , σ and φ are the viscosity and density of the continuous phase, the interfacial tension between the dispersed and aqueous phases and the dispersed phase volume fraction, respectively.

At high monomer conversion, where the polymerizing monomer-polymer particles behave like rigid spheres, the coalescence efficiency can be expressed as:

$$\lambda_c^{(\beta)}(V, U) = \exp\left(-a'_c \frac{\mu_c}{\rho_c \varepsilon_s^{1/3} (D_v + D_u)^{4/3}}\right) \quad (20)$$

In general, the monomer drops behave like deformable drops at the beginning of polymerization, while at high monomer conversion they behave like rigid polymer particles. Thus, the coalescence efficiency over the whole monomer conversion range can be written as:

$$\exp[-\lambda_c(V, U)] = \left\{ (1-\chi) \exp[-\lambda_c^{(\alpha)}(V, U)] \right\} + \left\{ \chi \exp[-\lambda_c^{(\beta)}(V, U)] \right\} \quad (21)$$

where χ is the fractional monomer conversion.

For high values of the dispersed phase volume fraction, the ‘damping’ effect of the dispersed phase on the local turbulent intensity needs to be taken into account by using effective viscosity of the dispersion

phase [7]:

$$\varepsilon_s / \varepsilon_c = (v_c / v_s)^3 \quad (22)$$

k_b , a_b , k_c , a_c and b_c are adjustable parameters and must be estimated.

2.2- Evaluation of the physical properties

The density of the suspension system, ρ_s , can be calculated as a weighted average of densities of the dispersed and continuous phases:

$$\rho_s = \rho_d \phi + \rho_c (1-\phi) \quad (23)$$

The density of the dispersed phase is in turn a function of the corresponding densities of the polymer and monomer and the extent of monomer conversion:

$$\rho_d = \left(\frac{\chi}{\rho_p} + \frac{1-\chi}{\rho_m} \right)^{-1} \quad (24)$$

The viscosity of the liquid (solid)-liquid dispersion phase was calculated by the following semi-empirical equation [1]:

$$\mu_s = \frac{\mu_c}{1-\phi} \left(1 + \frac{1.5 \mu_d \phi}{\mu_d + \mu_c} \right) \quad (25)$$

The variation of the viscosity of the polymerizable monomer phase was calculated using the following non-ideal mixing equation for the monomer/polymer solution [9]:

$$\ln \mu_d = (1-\phi_p) \ln \mu_m + \phi_p \ln \mu_p + \left[k_{m,p} + l_{m,p} (1-2\phi_p) \right] (1-\phi_p) \phi_p \left(\frac{\ln \mu_p - \ln \mu_m}{2} \right) \quad (26)$$

where ϕ_p is the volume fraction of the polymer in the dispersed phase and is given by following equation:

$$\phi_p = \chi \left(\frac{\rho_d}{\rho_p} \right) \quad (27)$$

$k_{m,p}$ and $l_{m,p}$ are model parameters. The change in the interfacial tension with respect to the stabilizer (PVA) concentration was calculated by the following equation:

$$\sigma = \sigma_0 - K_\sigma \frac{K_A C_{PVA}}{1 + K_A C_{PVA}} \quad (28)$$

The change in the interfacial tension with monomer conversion was taken into account according to the original work of Maggioris et al. [6]. K_σ and K_A are model parameters and σ_0 denotes the interfacial tension between the pure water phase and dispersed monomer phase, in the absence of a stabilizer.

3- Numerical solution of population balance equation

The numerical solution of PBE commonly requires the discretization of the particle volume domain into a number of discrete elements. Accordingly, the unknown number density function is approximated at a selected number of discrete points, resulting in a system of stiff, non-linear differential equations that is subsequently integrated numerically. Several numerical methods have been proposed in the literature for the solution of general PBE (Eq. (1)) in the continuous or equivalent discrete form. In the present study, the cell average technique (CAT) of Kumar et al. [10] was employed for

solving continuous PBE (Eq. (1)).

Following the original developments of Kumar et al. [10], the entire size domain is divided into a finite number of small cells. The lower and upper boundaries of the i th cell are denoted by $x_{i-1/2}$ and $x_{i+1/2}$ respectively. All particles belonging to a cell are identified by a representative size of the cell, also called grid point. The representative size of a cell can be chosen at any position between the lower and upper boundaries of the cell. In the original work of Kumar et al. [10], the centre of the cell, the arithmetic mean of the cell boundaries, is defined as the representative size. The discretized size domain is shown in Fig. 1.

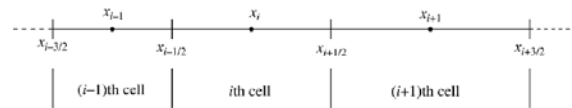


Figure 1. A discretized size domain

By integrating Eq. (1) over the discrete size interval $(x_{i-1/2}, x_{i+1/2})$ and properly accounting for the respective drop breakage and coalescence terms, the following set of discretized equations can be derived [10]:

$$B_{break,i}(t) = \sum_{k \geq i} N_k(t) g_k \int_{x_{i-1/2}}^{x_k} u(x) \beta(x, x_k) dx \quad (29)$$

$$De_{break,i}(t) = g_i N_i(t) \quad (30)$$

$$B_{coal,i}(t) = \sum_{\substack{j \geq k \\ x_{i-1/2} \leq (x_j + x_k) < x_{i+1/2}}} \left(1 - \frac{1}{2} \delta_{j,k} \right) k(x_j, x_k) N_j(t) N_k(t) \quad (31)$$

$$De_{coal,i}(t) = N_i(t) \sum_{k=1}^I k(x_i, x_k) N_k(t) \quad (32)$$

$$\frac{dN_i(t)}{dt} = B_{coal+break,i}^{CA}(t) - De_{coal+break,i}(t) \quad (33)$$

where the terms $B_{coal+break,i}^{CA}$ and $De_{coal+break,i}$ represent the birth and death rates of particles in the i th cell due to coalescence and breakage respectively. The total birth and death rates in i th cell is given by:

$$B_{coal+break,i} = B_{coal,i} + B_{break,i} \quad (34)$$

$$De_{coal+break,i} = De_{coal,i} + De_{break,i} \quad (35)$$

The modified birth term or the cell average birth term can then be computed as:

$$\begin{aligned} B_{coal+break,i}^{CA} = & B_{coal+break,i-1} \lambda_i^-(\bar{v}_{i-1}) H(\bar{v}_{i-1} - x_{i-1}) \\ & + B_{coal+break,i} \lambda_i^-(\bar{v}_i) H(x_i - \bar{v}_i) \\ & + B_{coal+break,i} \lambda_i^+(\bar{v}_i) H(\bar{v}_i - x_i) \\ & + B_{coal+break,i+1} \lambda_i^+(\bar{v}_{i+1}) H(x_{i+1} - \bar{v}_{i+1}) \end{aligned} \quad (36)$$

where

$$\bar{v}_i = \frac{V_{coal,i} + V_{break,i}}{B_{coal,i} + B_{break,i}} \quad (37)$$

and

$$V_{break,i} = \sum_{k \geq i} N_k(t) g_k \int_{x_{i-1/2}}^{x_k} x u(x) \beta(x, x_k) dx \quad (38)$$

$$\begin{aligned} V_{coal,i} = & \sum_{x_{i-1/2} \leq (x_j + x_k) < x_{i+1/2}}^{j \geq k} \left(1 - \frac{1}{2} \delta_{j,k} \right) \\ & k(x_j, x_k) N_j(t) N_k(t) (x_j + x_k) \end{aligned} \quad (39)$$

$$\lambda_i^\pm = \frac{x - x_{i \pm 1}}{x_i - x_{i \pm 1}} \quad (40)$$

For more details, readers are referred to Kumar et al. [10].

4- Results and discussion

The predictive capabilities of the applied model are demonstrated by comparison of model predictions with experimental data on average mean diameter and droplet/particle size distribution of both non-reactive liquid-liquid dispersions of styrene in water [11] and free-radical suspension polymerization of styrene [12]. The PSD model used in the present work was solved together with a comprehensive dynamic kinetic model, describing the polymerization rate and monomer conversion of styrene in a batch suspension polymerization reactor [13]. The physical and transport parameters, appearing in the PSD model of the styrene suspension polymerization system, are reported in Table 1. All simulations were carried out in a 4-baffled CSTR equipped with a 6-blade disk turbine agitator. The reactor internal diameter and height are 14.4 cm. The ratio of the impeller clearance above the reactor bottom to the reactor height is 0.5 and the power number is equal to 5.

The dynamic evolution of styrene droplet size distribution (DSD) in aqueous dispersion was experimentally studied by Yang et al. [11]. Fig. 2 illustrates the model prediction of the dynamic evolution of the Sauter mean diameter of styrene droplets for two different monomer volume fractions. The temperature was kept constant at 25°C, the agitation speed was 350 rpm, while 0.5 (gr/L) of PVA was added to the aqueous phase for stabilization of the dispersion. The PVA had a degree of hydrolysis equal to 87-89 %, while its molecular weight varied between 30,000 and 50,000 (gr/mol). As can be seen from Fig. 2 there is a good agreement between the experimental data [11] and

model prediction. Fig.3 shows the model prediction of the effect of agitation rate on

the steady-state DSD of the styrene droplets. The monomer volume fraction was set to 0.1.

Table 1. Physical and transport properties

Physical, transport properties for Styrene/PS system	References
$\rho_m = 923.6 - 0.887(T - 273.15)$ (Kg / m ³)	[1]
$\rho_p = 1050 - 0.602(T - 273.15)$ (Kg / m ³)	[1]
$\mu_m = \exp\left(-22.673 + \left(\frac{1758}{T}\right) + 1.67 \ln(T)\right)$ (Pa.s)	[13]
$E_p = 3.38 \times 10^9$ (Kg / m.s ²)	[1]
$k_{m,p} = -1.7649, l_{m,p} = 1.8556$	[9]
$K_\sigma = 15.088, K_A = 0.46$	This study
$a_b = 2.5 \times 10^{-9}, k_b = 1.3 \times 10^{-9}, a_c = 8 \times 10^{13}, a'_c = 550, k_c = 1.3 \times 10^4, r = 35, S_{Nsa} = 25$	This study

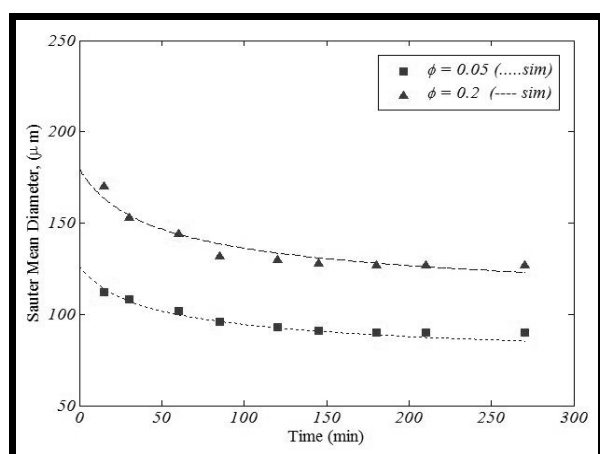


Figure 2. Dynamic evolution of Sauter means Diameter of styrene droplets (Experimental data point: [11])

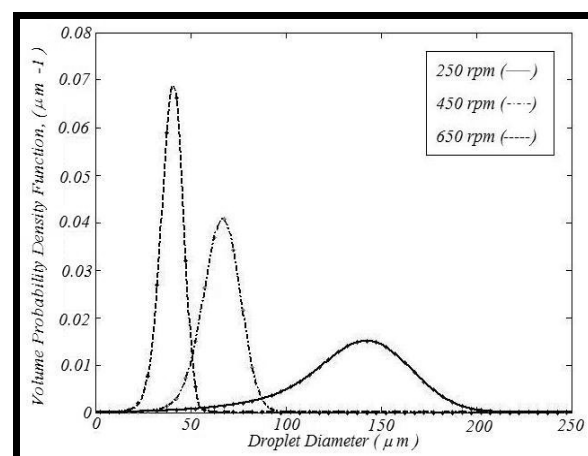


Figure 3. Effect of agitation rate on distributions of styrene droplets

Figs. 4 and 5 show the model prediction of a time-conversion curve for free-radical suspension polymerization of styrene and the change of dispersed phase viscosity during the reaction. The temperature was kept at 60°C and 0.01 (mol/L) of AIBME was used as the initiator in suspension polymerization of styrene. As can be seen, there is a good agreement between the experimental data [13] and the simulation results in Fig. 4.

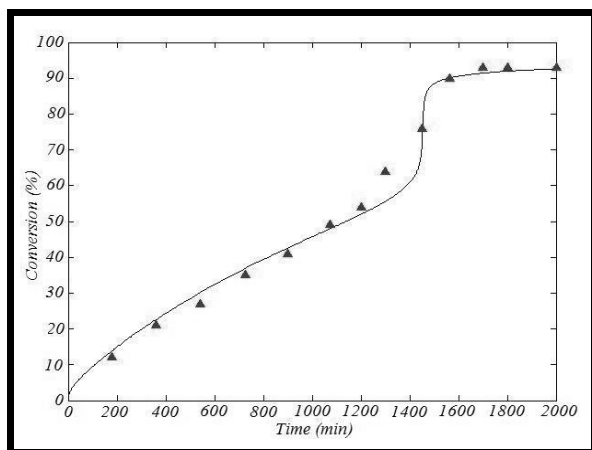


Figure 4. Conversion versus time for AIBME-Initiated suspension polymerization of styrene (experimental data points: [13])

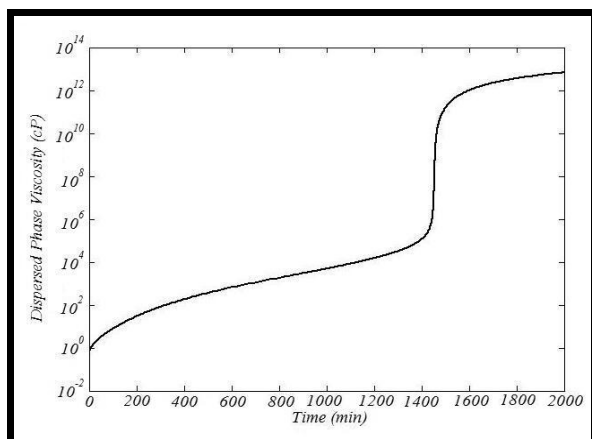


Figure 5. Dispersed phase viscosity versus time for AIBME-Initiated suspension polymerization of styrene (model Prediction)

The present model was employed to predict the dynamic evolution of PSD in the free-radical suspension polymerization of styrene. More specifically, the effects of agitation rate and temperature on the PSD were investigated for the polystyrene suspension polymerization process. Fig. 6 shows the dynamic evolution of the mean diameter of styrene/polystyrene particles. The temperature was kept at 70°C and 0.05 (mol/L) of AIBN was used as the initiator in the suspension polymerization of styrene. The agitation speed was 240 rpm, while 1 (gr/L) of PVA was added to the aqueous phase for stabilization of the dispersion. The dynamic evolution of styrene/ polystyrene particle size distribution (PSD) in aqueous dispersion was experimentally studied by Konno et al. [12]. As can be seen from Fig. 6 and Fig. 7, there is good agreement between the experimental [12] and model prediction.

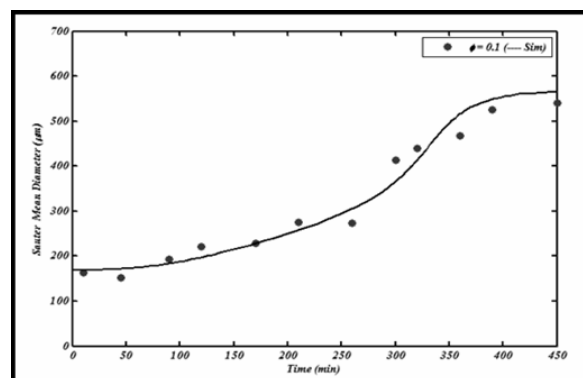


Figure 6. Dynamic evolution of Sauter mean diameter of styrene /polystyrene (experimental data points: [12])

Fig. 8 illustrates the effect of the agitation rate on the final PSD of polystyrene particles. Fig. 9 shows the effect of temperature on the dynamic evolution of the mean diameter of styrene/polystyrene particles. As can be seen

the mean size of polystyrene particles increases with temperature. This can be explained as discussed below. By increasing the temperature, the rate of polymerization is increased, resulting in a higher viscosity of drops. The rise in drop viscosity leads to a decrease of drop breakage and an increase in drop coalescence rates, resulting in a larger particle size. The agitation speed was 240 rpm, and 0.05 (mol/L) of AIBN was used as initiator and 1 (gr/L) of PVA was added to the aqueous phase to stabilize the dispersion.

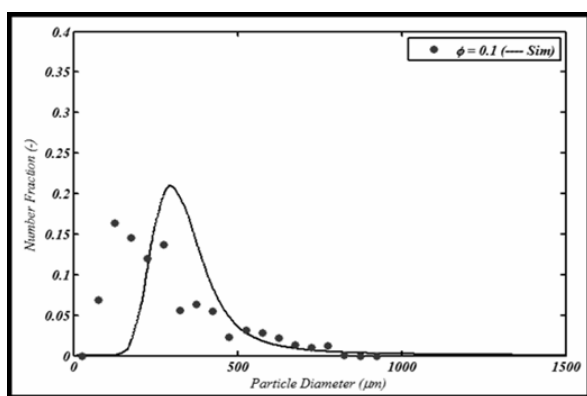


Figure 7. Final particle size distribution of polystyrene (experimental Data points: [12])

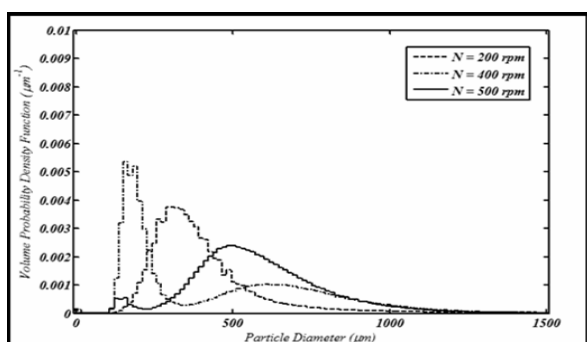


Figure 8. Effect of agitation rate on distributions of polystyrene particles

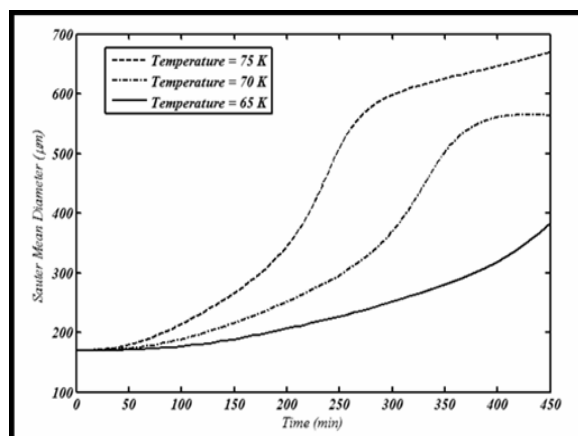


Figure 9. dynamic evolution of Sauter mean diameter of polystyrene

5- Conclusions

In this study a model presented in the literature has been used for prediction of droplet/particle size and size distribution, conversion of monomer in liquid-liquid dispersion of styrene in water, and the suspension polymerization of styrene. The cell average technique has been used for solving the population balance equation. Model predictions have been compared with the experimental data available in the literature. Computer simulation indicates that there is a good agreement between the experimental data and the simulation results, which means that the selected model has a good capability in predicting polymer conversion, particle mean size and polymer particle size distribution.

6- Nomenclature

- a_b, a_c adjustable parameters
- b_c adjustable parameters
- B birth rate, $1/m^3$
- C_{PVA} concentration of surface-active agent, Kg/m^3
- D diameter, m
- De death rate, $1/m^3$

E	elasticity modulus, Kg/m s ²
$g(V)$	breakage rate, 1/s
I	total number of cells
$k(V, U)$	coalescence rate, m ³ /s
$k_b, k_c, k_{m,p}, k_A, k_\sigma$	adjustable parameters
$l_{m,p}$	adjustable parameters
L	macroscale of turbulence, m
$n(V, t)$	number density function, 1/m ⁶
$N_i(t)$	number of particles having volume equal to x_i per reactor unit volume, 1/m ³
Re	Reynolds number
t	Time, s
T	Temperature, K
$u(V)$	number of droplets formed by breakage of a droplet of volume V
$\bar{u}(D_v)$	mean square of the relative velocity between two points separated by a distance D , m/s
V, U, x	volumes, m ³
Ve	elasticity parameter
We	Weber number

Greek letters

$\beta(U, V)$	daughter droplets probability function, 1/m ³
δ_{ij}	Kronecker delta
ε	average energy dissipation rate per unit mass, m ² /s ³
η	microscale of turbulence, m
λ_b, λ_c	breakage and coalescence efficiencies
μ	viscosity, Kg/m s
ν	kinematic viscosity, m ² /s
ρ	density, Kg/m ³
σ	interfacial tension, Kg/s ²
σ_0	interfacial tension between pure water and the dispersed phase, Kg/s ²
ϕ	dispersed phase volume fraction

ϕ_p	volume fraction of the polymer in the dispersed phase
χ	monomer conversion
ω_b, ω_c	breakage and coalescence frequencies, 1/s
Ω	efficiency parameter

Subscripts

c	continuous phase
d	dispersed phase
m	monomer
P	polymer
S	suspension system

Superscripts

CA	cell average
------	--------------

References

- [1] Kotoulas, C., and Kiparissides, C., "A generalized population balance model for the prediction of particle size distribution in suspension polymerization reactors", Chem. Eng. Sci., 61, 332(2006).
- [2] Saliakas, V., Kotoulas, C., Meimaroglou, D., and Kiparissides, C., "Dynamic evolution of the particle size distribution in suspension polymerization reactors: a comparative study on monte carlo and sectional grid methods", Can. J. Chem. Eng., 86, 924(2008).
- [3] Jahanzad, F., Sajjadi, S., and Brooks, W. B., "Characteristic intervals in suspension polymerization reactors: an experimental and modelling study", Chem. Eng. Sci., 60, 5574(2005).
- [4] Alvarez, J., Alvarez, J., and Hernandez, M., "A population balance approach for the description of particle size distribution in suspension polymerization reactors", Chem. Eng. Sci., 49(1), 99(1994).

- [5] Chen, Z., Pauer, W., Moritz, H.-U., Pruss, J., and Warnecke, H. J., "Modeling of the suspension polymerization process using a particle population balance", *Chem. Eng. Technol.*, 22, 609(1999).
- [6] Maggioris, D., Goulas, A., Alexopoulos, A.H., Chatzi, E.G., and Kiparissides, C., "Prediction of particle size distribution in suspension polymerization reactors: effect of turbulence nonhomogeneity", *Chem. Eng. Sci.*, 55, 4611(2000).
- [7] Doulah, M.S., "An effect of hold-up on drop sizes in liquid-liquid dispersions", *Ind. Eng. Chem. Fundamen.*, 14(2), 137(1975).
- [8] Coualoglou, C.A., and Tavlarides, L.L., "Description of interaction processes in agitated liquid-liquid dispersions", *Chem. Eng. Sci.*, 32, 1289(1977).
- [9] Song, Y., Mathias, P.M., Tremblay, D., and Chen, C.C., "Liquid Viscosity model for polymer solutions and mixtures", *Ind. Eng. Chem. Res.*, 42, 2415(2003).
- [10] Kumar, J., Peglow, M., Warnecke, G., and Heinrich, S., "An efficient numerical technique for solving population balance equation involving aggregation, breakage, growth and nucleation", *Powder Technology*, 182, 81(2008).
- [11] Yang, B., Takahashi, K., and Takeishi, M., "Styrene drop size and size distribution in an aqueous solution of poly(vinyl alcohol)", *Ind. Eng. Chem. Res.*, 39, 2085(2000).
- [12] Konno, M., Arai, K., and Saito, S., "The effect of stabilizer on coalescence of dispersed drops in suspension polymerization of styrene", *Journal of Chem. Eng. Of Japan*, 15(2), 131(1982).
- [13] Achilias, D.S., and Kiparissides, C., "Development of a general mathematical framework for modelling diffusion-controlled free-radical polymerization reactions", *Macromolecules*, 25(14), 3739(1992).
- [14] Olayo, R., Garcia, E., Garcia-Corichi, B., Sanchez-Vazquez, L., "Poly(vinyl alcohol) as a stabilizer in the suspension polymerization of styrene: the effect of the molecular weight", *Journal of Applied Polymer Science*, 67, 71, (1998).